HEATING AND COOLING IN HIGH-RISE BUILDINGS USING FAÇADE-INTEGRATED TRANSPARENT SOLAR THERMAL COLLECTOR SYSTEMS

Christoph Maurer[1], Thomas Baumann[2], Michael Hermann[1], Paolo Di Lauro[1], Stefano Pavan[3], Lars Michel[4], and Tilmann E. Kuhn[1]
[1]Fraunhofer Institute for Solar Energy Systems, Freiburg, Germany
[2]Peter Berchtold, Ing.-Büro, Sarnen, Switzerland / IPB GmbH, Frankfurt, Germany
[3]Permasteelisa S.p.A, Treviso, Italy
[4]Interpane Entwicklungs- und Beratungsgesellschaft, Lauenförde, Germany

ABSTRACT

New façades of high-rise buildings often include renewable energy converters to allow "green building" operation. At the same time, numerous tenants value visual transparency. Transparent solar thermal collectors (TSTC) aim at decreasing the non-renewable primary energy (NRPE) demand and increasing the visual transparency at the same time. On the one hand, this paper presents the main modelling challenges that arise when considering building façades and especially integrated TSTC systems. New TRNSYS Types have been especially developed for this purpose. A simplified model is presented for comparison. On the other hand, the overall performance for a building with façade-integrated TSTC, as measured by its NRPE demand, is treated. This is achieved by considering a complete simulation model coupling the TSTC, building and HVAC operation. Possibilities for PE savings are investigated using the building mass as additional thermal storage.

INTRODUCTION

"Green" or "sustainably built" buildings are an obvious major topic of interest today (resource usage reduction, greenhouse gas emission reduction, …). The background motivation to this paper is the reduction of the non-renewable primary energy (NRPE) demand in high-rise buildings. A particular type of clean energy-producing equipment is investigated, which can be incorporated into the building façade. Thus, it does not require large roof and/or unused outdoor areas which are not available in the case of a high-rise building. The transparent solar thermal collector is not only interesting because of its façade integration capability but also because of its visual transparency. The visual transparency of the façade is generally very positively valued by tenants, as indicated by modern architectural projects. The challenge of predicting the primary energy demand using transparent collectors has many dimensions. The solar transmission has to be modelled with a high accuracy also for diffuse radiation. The g-value – also called "solar factor", "solar heat gain coefficient (SHGC)" and "total solar energy transmittance" (TSET) – cannot be considered as a constant value, but depends also on the collector operation. (Maurer and Kuhn 2011) presented a new detailed collector model and a connection to a building in TRNSYS and offer an advanced calculation method for glazing with blinds with a second BlackBoxType. The first simulation part focuses on a comparison of the new detailed collector model with a simplified one. The second part then presents coupled simulations of a building with a collector and an HVAC system including solar cooling, focusing on asynchronous demand and renewable supply.

SIMULATION

Setting

For both simulation parts, a 40-storey high-rise building with a square floor plan 46x46m^2, which is presented in Figure 1(a), was considered. A simple layout with 4 times 12 cell offices with a ground area of 3x8m^2 each was chosen. A cell office has an opaque wall section of 1m height which covers the floor slab and the thickness of the floor. In the visual area, windows with a height of 1.5m are placed as shown in Figure 1(b). The 1.25m high spandrel area is equipped with transparent solar thermal collectors like the test model shown in Figure 2. The collector occupies 26 % of the total façade area. Frankfurt am Main was chosen as the location for the meteorological data.

Façade areas other than cell office front façades are modelled adiabatically (corridor façade and cell office side façade). Computing time can then be reduced by scaling the storey down by a factor of 12. Each storey has 300 m^2 corridor area, a 364 m^2 core, four 51 m^2 meeting rooms, two 28 m^2 copier rooms and two 20 m^2 kitchen areas. Typical internal loads were assumed.

The building façade parameters have been chosen as follows to obtain a high-performance façade:

- opaque façade U value: 0.25 W/m^{2}K
- window U value : 1.2 W/m^{2}K
- glazing g-value (⊥): 0.28
- g-value of glazing with fully closed shading (⊥): 0.14

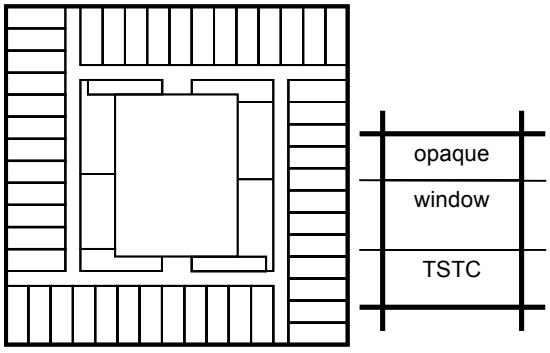

(a) (b)

Figure 1 (a) Floor plan and (b) façade layout of one cell office with an opaque area, a window in the visual area and transparent solar thermal collectors (TSTC) in the spandrel area.

Figure 2 Picture of a TSTC test model.

Detailed façade model for transparent collectors

As presented in (Maurer and Kuhn 2011), Type 871 is the implementation of a one-dimensional multi-layer model in TRNSYS. This model calculates the effective solar absorptances and transmittance based on angle-dependent spectrally resolved polarized input data for each layer of a transparent façade component. While the model can be used to represent a large variety of transparent façade components, Type 871 is the implementation of a specific TSTC design in the general detailed model. Together with an integrated radiation processor based on (Tregenza 1987; Perez, Seals, and Michalsky 1993; Reinhart and Walkenhorst 2001), even the diffuse radiation is calculated with high accuracy. The internal heat transfer is calculated with temperature-dependent formulas for radiation and convection which leads to temperature-dependent U values. A matched flow control is implemented to reach a chosen target temperature whenever this is possible. For this paper we modelled a TSTC with three glass panes, one transparent absorber and argon filling.

Simplified façade model for transparent collectors

In this publication we present a simplified façade model which is actually the most advanced model for transparent collectors which we were able to implement with state-of-the-art TRNSYS Types. Nevertheless, the detailed TSTC model was used to derive the parameters for the simplified model. Type71 was used to model the TSTC with 2D IAM input data based on the angle-dependent spectrally resolved polarized optical simulation of Type 871. This data is also the basis for calculation of the solar transmittances of diffuse sky and ground radiation. The value of the diffuse sky transmittance was also used for the transmittance of direct radiation. Type 871 was further used to derive a U value of 0.6 W/(m^{2}K) for the simplified model as well as a secondary solar heat gain q_i of 0.056 based on the assumption of 500 W/m^2 irradiation, an average fluid temperatue of 75°C and an ambient and room temperature of 25°C. Type 871 was also used to determined a collector efficiency curve with parameters η_0 = 0.60, a_1 = 2.86 W/(m^{2}K) and a_2 = 0.006 W/(m^{2}K^2). For commercial collectors, measured efficiency parameters will be available and Type871 will reproduce the measurements. The heat flow into the building was calculated by:

$$Q_{\text{int}} = q_i G - U(T_{room} - T_a) \qquad (1)$$

Façade model for glazing and blinds

Type 861 is a TRNSYS implementation of the black box model presented by (Kuhn et al. 2011). This model uses bidirectional input data of the transmittance, the g-value and the reflectance. While the implementation in ESP-r still used average values for the diffuse sky and ground radiation, the Type861 treats 235 patches of the unity sphere individually. A cut-off control is implemented for the blind, which blocks all direct radiation while minimizing the slat tilt angle. At irradiance values below 150 W/m^2, the blinds are fully retracted.

Connection to the building

To connect the façade Types 861, 871 and the simplified façade model to the building Type 56, a modified window is used. A high thermal resistance between the exterior and the interior pane first minimizes the influence of the ambient temperature. The heat transfer to the interior calculated by a façade Type can then be introduced as a wall gain on the interior pane. The solar transmission calculated by a façade Type is introduced as radiation using a new orientation and a solar direct transmittance of 1.

This approach models the interior surface with respect to both the dimensions and temperature, so that thermal comfort can be assessed in future.

HVAC system

A thermally activated building system has been considered to provide the space heating and cooling (slab surface activation). A ventilation system with highly efficient heat recovery provides the hygienically necessary air change. The ventilation system has been modelled to supply fully conditioned air (temperature and humidity). The room comfort conditions are standard with reference to ISO 7730 and DIN 13779.

The central HVAC system integrates the TSTCs into a collector network supplying a central thermal storage buffer (Baumann, Tammler, and Reber 2010). The buffer supplies heat to the heating devices as well as a sorption chiller and is one of the core elements of the HVAC system. To cover the loads that cannot be met by the solar collectors / sorption chiller, a compression chiller is used on the cooling side and a gas boiler on the heating side. Furthermore, hybrid coolers are used to disperse the excess heat of the chillers. The hybrid coolers are also used in a free cooling mode for the TABS cooling when outside temperatures permit this.

The strategy for controlling the HVAC system is as follows:

The solar thermal energy provided by the TSTCs is stored continuously in the buffer and provided to the users. The lower the buffer temperature, the better the efficiency of the collectors. The minimum temperatures that have been defined are 36°C for the supply of the heating system (from October to April) and 80°C for the supply of the sorption chiller (from May to September).

If the collector energy is not needed, the temperature level in the buffer is raised and/or the temperature level in the building is lowered or raised within the user comfort limits, thereby exploiting the storage capacity of the building. As a last resort, the heat produced by the collector is released via the hybrid coolers.

DISCUSSION AND RESULT ANALYSIS

Detailed vs. simplified façade model

For the comparison between the detailed Type 871 and the simplified model for transparent collectors, a slightly different space heating/cooling configuration was considered (heating/cooling floor convectors instead of TABS). The reason for this choice is that the thermally faster reacting convectors allow the effects to be shown more directly than TABS.

The values in Table 1 demonstrate that the heating and cooling load can be approximated well using the simplified TSTC model, while the collector gain is underestimated by about 15%.

Table 2 presents a comparison of the solar transmission through the TSTC and the heat transfer from the TSTC to the building. During the heating season, the solar transmission and the heat flux into the building are underestimated. The annual heating load is therefore slightly overestimated.

During the cooling season, the simplified model slightly overestimates the solar transmission, but considerably underestimated the heat flux into the building. The two errors partly compensate each other, so the annual cooling load is only underestimated by about 5%.

Figure 3 illustrates how underestimations and overestimations can either compensate or add to each other. The heating load differences between the simplified and the detailed model range from -0.9 to +1.5 W for a one-hour time step, the cooling load differences from -2 to +1.3 kW and the collector gain from -6.5 to +2.7 kW.

Table 1
Annual values for one storey with the detailed and simplified TSTC models

TSTC MODEL	HEATING LOAD [Wh]	COOLING LOAD [Wh]	COLLECT-OR GAIN [Wh]
Detailed	2.33E+07	2.55E+07	1.68E+07
Simplified	2.36E+07	2.42E+07	1.43E+07

Table 2
Annual values for the collectors of one storey with the detailed and simplified TSTC models

TSTC MODEL	SOLAR TRANSMIS-SION [Wh]	HEAT TRANSFER TO BUILDING INTERIOR [Wh]
Detailed, heating season	1.24E+06	-4.06E+06
Simplified, heating season	1.19E+06	-4.61E+06
Detailed, cooling season	1.76E+06	2.33E+06
Simplified, cooling season	1.87E+06	9.80E+05

Moreover, these values are only valid for the presented operation mode. Figure 4 presents the heat transfer from the collectors of the west façade to the interior for one day in May. The heat transfer to the interior is overestimated or underestimated depending on the collector operation mode. Before 8 a.m. and after 5 p.m., there is no fluid flow, but already a difference between the detailed and simplified models occurs. Also at night, the temperature-dependent U value of the detailed model leads to differences. Between 8 a.m. and 5 p.m., a constant secondary solar heat gain q_i cannot reflect different operation modes, because the heat transfer to the interior depends on the amount of

extracted collector gain, which is inherently time dependent.

To assess the approximation for the collector gain by the simplified model, Figure 5 and Figure 6 present comparisons for two days in March. Figure 5 presents a day with a high fraction of direct radiation and Figure 6 a day with a high fraction of diffuse radiation. The results show that the simplified model can handle direct radiation with small relative errors, but the relative errors increase with an increasing fraction of diffuse radiation.

The simplified model can therefore only be recommended as an approximation for TSTC if its parameters are chosen very carefully, if minimum computing times are required and if the HVAC control is not targeted.

Solar-thermal heating / cooling

Thermal energy storage is essential in systems which make efficient use of solar energy. Tables 3, 4 and 5 show how the buffer storage capacity affects the efficiency of the collector / HVAC system.

It is also clearly evident that the solar-thermal heat production is reduced substantially as the buffer size is reduced and the average working temperature rises.

The option of using the building mass actively for heat storage is shown to be interesting as it allows precious space to be saved, which would otherwise be needed for heat storage tanks. The drawback of such a solution is greater complexity on the control systems side.

To summarise, a 26% façade coverage with TSTC on east, west and south façades allows approximately 20% of the total heating and cooling energy demand of a high-rise building to be met with renewable energy.

A comparison between solar thermal cooling and solar electrical cooling using photovoltaic modules always depends on the target application (Hartmann, Glueck, and Schmidt 2011; Henning and Wiemken 2011; Fong et al. 2010). With the right formulas, a detailed façade model for building-integrated photovoltaics (BIPV) including transparent BIPV can be established in the future.

CONCLUSION

Simplified transparent collector models cannot reproduce the complex behaviour of the solar transmission and the heat transfer to the building interior adequately. Even an advanced simplified model with carefully chosen parameters underestimates the annual collector gain by 15% and overestimates the heat transfer to the building interior by a factor of 2. The quality of the approximation of the collector gain decreases with an increasing fraction of diffuse radiation.

It is shown that equipping façades with transparent solar thermal collectors allows substantial renewable energy gains. A double benefit is thus attained with these elements, which provide better visual contact to the exterior as a consequence of their transparency.

Table 3
Utilisation of solar energy available from the collector and solar fraction of heating / cooling load

STORAGE BUFFER VOLUME [m^3]	SOLAR USAGE[1] [%]	SOLAR FRACTION[2] OF H/C LOAD [%]
500	95	21
250	89	20
100	82	18
50	80	17
50 and building mass	90	21

ACKNOWLEDGEMENTS

The research leading to these results has received funding from the European Community's Seventh Framework Programme under grant agreement n° 212206. C. Maurer thanks the German National Academic Foundation for support.

NOMENCLATURE

SYMBOL	EXPLANATION
a_1, a_2	Collector efficiency coefficients (W/(m^{2}K), W/(m^{2}K^2))
α_s	Solar altitude angle
F'	Collector efficiency factor
G	Solar irradiance (W/m^2)
γ	Façade orientation (0° south, west positive)
γ_s	Solar azimuth angle (0° south, west positive)
γ_f	$\gamma_f = \gamma_s - \gamma$, façade azimuth angle (0° parallel to façade normal)
IAM	Incidence angle modifier
η, η_0	Collector efficiency $\eta=\eta_0-a_1x-a_2x^2G$, collector efficiency at x=0
Q_{use}	Collector gain (W)

[1] The solar (energy) utilisation of the system is defined here as the ratio between the solar energy processed in the HVAC system for heating and cooling purposes and the net solar energy available at the collector output over a period of one year.

[2] The solar (energy) fraction of the system is defined here as the ratio between the solar energy contributing to meeting the building heating / cooling load and the total building heating / cooling load referenced in heat either for direct usage or for processing via a sorption chiller.

Q_{int}	Heat transfer from the collector to the room (W/m^2)
q_i	Secondary solar heat gain
TSTC	Transparent solar thermal collector
T_a, T_{room}	Ambient temperature, room air temperature (K)
U	U value (W/m^2K)
x	Difference between the ambient temperature and the average fluid temperature divided by the solar irradiance (m^2K/W)

REFERENCES

Baumann, Thomas, Nina Tammler, and Jan Reber. 2010. *Solar heating and cooling in high rise buildings - HVAC and building simulation report for EU project Cost-Effective Task 3.1*. Personal communication. Frankfurt: IPB GmbH, Ingenieurgesellschaft für Energie- und Gebäudetechnik.

Fong, K.F., T.T. Chow, C.K. Lee, Z. Lin, and L.S. Chan. 2010. Comparative study of different solar cooling systems for buildings in subtropical city. *Solar Energy* 84, no. 2 (February): 227-244.

Hartmann, N., C. Glueck, and F.P. Schmidt. 2011. Solar cooling for small office buildings: Comparison of solar thermal and photovoltaic options for two different European climates. *Renewable Energy* 36, no. 5 (May): 1329-1338.

Henning, Hans-Martin, and Edo Wiemken. 2011. Heizen und Kühlen mit Sonnenenergie - Lösungsansätze auf Basis thermischer und elektrischer Verfahren. In *21. Symposium Thermische Solarenergie*. Regensburg: OTTI, May 12.

Kühn, Stefan. 1996. Modellierung von transparenten Wärmedämmmaterialien auf der Basis spektraler Daten. Freiburg: Universität Freiburg i. Br., Fraunhofer ISE.

Kuhn, Tilmann E., Sebastian Herkel, Francesco Frontini, Paul Strachan, and Georgios Kokogiannakis. 2011. Solar control: A general method for modelling of solar gains through complex facades in building simulation programs. *Energy and Buildings* 43, no. 1: 19-27.

Maurer, Christoph, and Tilmann E. Kuhn. 2011. Variable g-value of transparent façade collectors. *Energy and Buildings* Submitted.

Perez, R., R. Seals, and J. Michalsky. 1993. All-weather model for sky luminance distribution. Preliminary configuration and validation. *Solar Energy* 50, no. 3: 235-245.

Reinhart, Christoph F., and Oliver Walkenhorst. 2001. Validation of dynamic RADIANCE-based daylight simulations for a test office with external blinds. Energy and Buildings 33, no. 7: 683-697.

Tregenza, P. R. 1987. Subdivision of the sky hemisphere for luminance measurements. *Lighting Research and Technology* 19: 13-14.

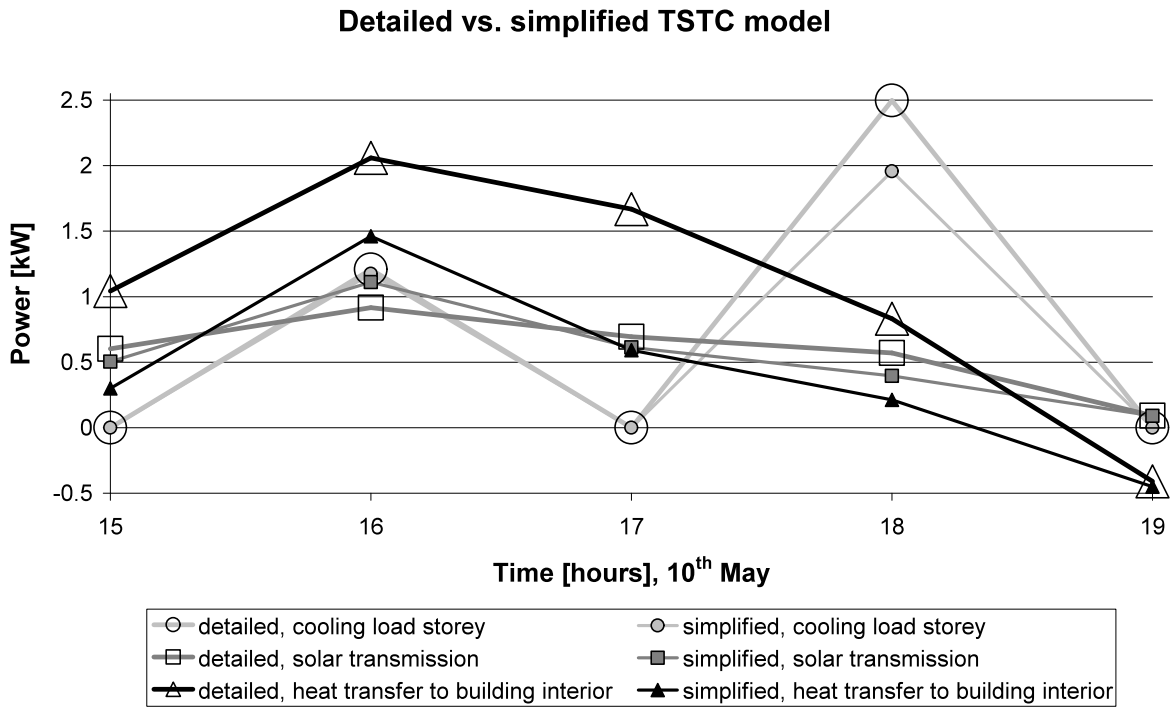

Figure 3 Comparison of the detailed and the simplified TSTC model for the collectors and the cooling load of one storey.

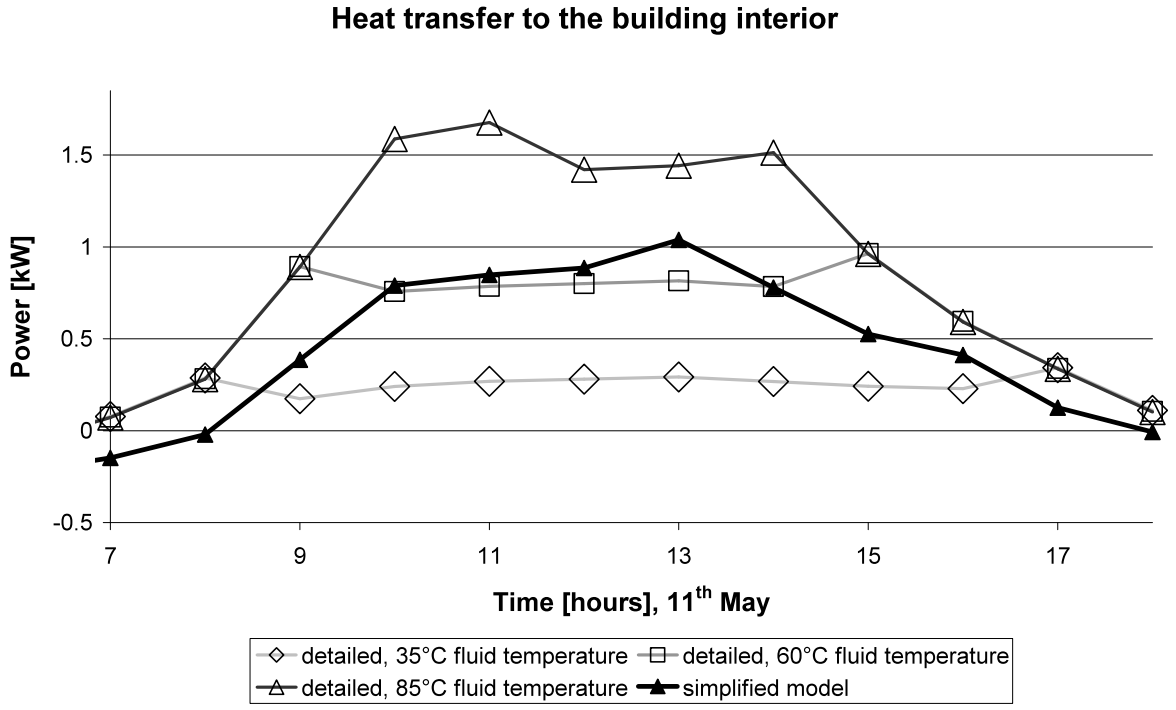

Figure 4 Heat transfer from the collectors of the south facade to the building interior for different façade models and different average fluid temperatures during operation.

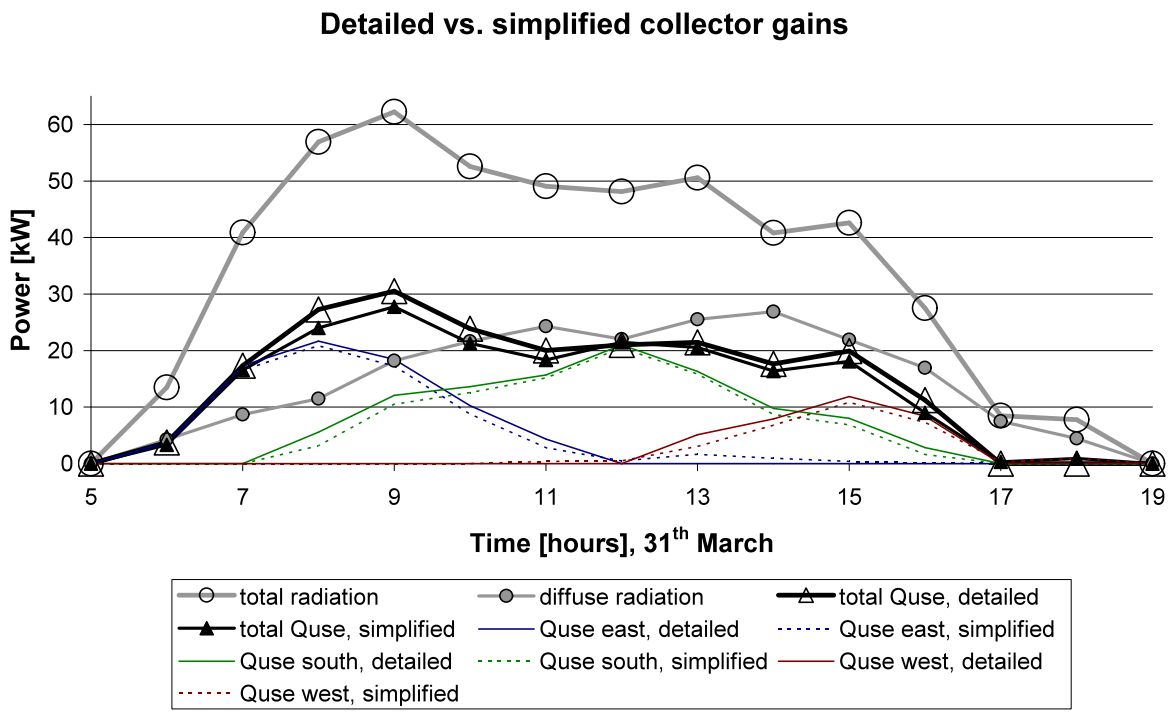

Figure 5 Comparison of the total collector gain Quse of one storey for a high fraction of direct irradiance. The contributions of the TSTC on the east, south and west façades are indicated.

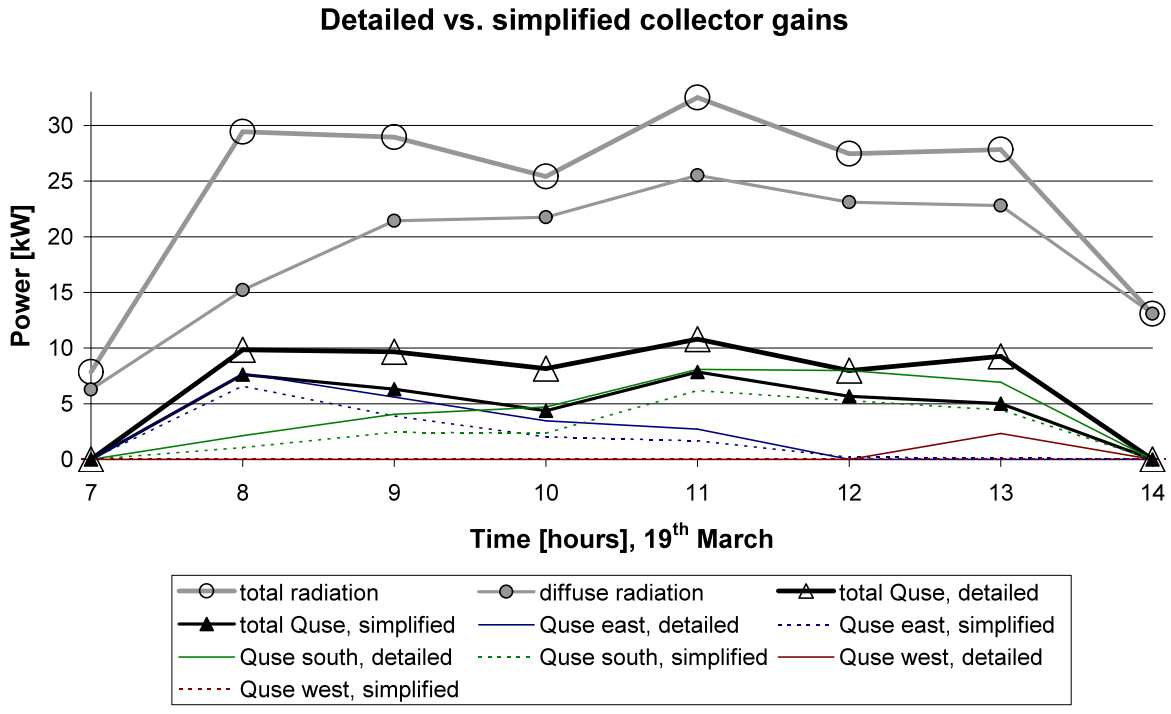

Figure 6 C Comparison of the total collector gain Quse of one storey for a high fraction of diffuse irradiance. The contributions of the TSTC on the east, south and west façades are indicated.

Table 4
Solar heat production and use for different heat storage capacities[3]
Annual values for the building

	STORAGE BUFFER VOLUME 500 [m³]		**STORAGE BUFFER VOLUME 250 [m³]**		**STORAGE BUFFER VOLUME 100 [m³]**		**STORAGE BUFFER VOLUME 50 [m³]**		**STORAGE BUFFER VOLUME 50 [m³] AND BUILDING MASS**	
	HEAT [kWh]	**PERCENTAGE [%]**	**HEAT [kWh]**	**PERCENTAGE [%]**	**HEAT [kWh]**	**PERCENTAGE [%]**	**HEAT [kWh]**	**PERCENTAGE [%]**	**HEAT [kWh]**	**PERCENTAGE [%]**
Heating	2.42E+05	46	2.17E+05	43	1.88E+05	39	1.68E+05	36	2.23E+05	42
Sorption chiller	2.27E+05	43	2.25E+05	45	2.09E+05	43	2.00E+05	42	2.52E+05	47
Rejected	2.55E+04	5	4.19E+04	8	7.76E+04	16	9.62E+04	20	5.20E+04	10
Losses	3.35E+04	6	2.20E+04	4	1.01E+04	2	7.19E+03	2	8.03E+03	2
Total solar	5.28E+05	100	5.06E+05	100	4.84E+05	100	4.72E+05	100	5.35E+05	100

Table 5
Heating and cooling load coverage for different heat storage capacities
Annual values for the building

	STORAGE BUFFER VOLUME 500 [m³]		**STORAGE BUFFER VOLUME 250 [m³]**		**STORAGE BUFFER VOLUME 100 [m³]**		**STORAGE BUFFER VOLUME 50 [m³]**		**STORAGE BUFFER VOLUME 50 [m³] AND BUILDING MASS**	
	HEAT [kWh]	**PERCENTAGE [%]**	**HEAT [kWh]**	**PERCENTAGE [%]**	**HEAT [kWh]**	**PERCENTAGE [%]**	**HEAT [kWh]**	**PERCENTAGE [%]**	**HEAT [kWh]**	**PERCENTAGE [%]**
Solar Heating	2.42E+05	29	2.17E+05	26	1.88E+05	23	1.68E+05	20	2.23E+05	27
Boiler	5.92E+05	71	6.16E+05	74	6.44E+05	77	6.65E+05	80	6.10E+05	73
Total heating	8.33E+05	100	8.33E+05	100	8.33E+05	100	8.33E+05	100	8.33E+05	100
	HEAT [kWh]	**PERCENTAGE [%]**	**HEAT [kWh]**	**PERCENTAGE [%]**	**HEAT [kWh]**	**PERCENTAGE [%]**	**HEAT [kWh]**	**PERCENTAGE [%]**	**HEAT [kWh]**	**PERCENTAGE [%]**
Sorption chiller	1.67E+05	16	1.66E+05	16	1.54E+05	15	1.47E+05	14	1.84E+05	18
Free cooling	6.55E+04	6	6.45E+04	6	6.57E+04	6	6.45E+04	6	6.45E+04	6
Compression chiller	7.90E+05	77	7.94E+05	78	8.05E+05	79	8.14E+05	79	7.74E+05	76
Total cooling	1.02E+06	100	1.02E+06	100	1.02E+06	100	1.02E+06	100	1.02E+06	100

[3] Compared to Figure 2, the control strategy was optimized with increased storage temperatures in times of low demand.